Consequences of asymmetric pumping in low pressure plasma processing reactors: A three-dimensional modeling study

Mark J. Kushner[a)]

University of Illinois, Department of Electrical and Computer Engineering, 1406 W. Green St., Urbana, Illinois 61801

Low pressure ($<$10s mTorr), high plasma density ($>10^{11}$ cm^{-3}) reactors are rapidly becoming the tool of choice for etching during microelectronics fabrication. Although gas injection and pumping are well characterized process parameters in higher pressure systems, the impact of the symmetry of gas injection and pumping on the uniformity of reactant fluxes to the substrate are less well known in low pressure systems. In this article, results from a three-dimensional plasma equipment model are used to investigate the consequences of asymmetric gas pumping on reactive fluxes in inductively coupled plasma reactors operating in Cl$_2$. We find that for typical conditions (10 mTorr, 150 sccm, 400 W) the azimuthal symmetry of ion density and ion fluxes are little affected by, for example, side pumping. This results from the dominance of ambipolar electric fields which are largely determined by the uniformity of ion sources and shape of the chamber. Neutral reactant fluxes do suffer azimuthal asymmetries due to pumping, however the variations are typically $<10\%-15\%$ over a pressure range of 5–20 mTorr. The magnitude of the side-to-side variations is largely determined by the relative rates of loss of reactant species to surfaces compared to pumping. © *1997 American Institute of Physics.* [S0021-8979(97)01723-4]

I. INTRODUCTION

It is well known that symmetric gas injection and pumping, and reactant generation, are required to obtain uniform reactant fluxes in high pressure ($>$100s mTorr) plasma etching and deposition systems for microelectronics fabrication. The consequences of asymmetric gas injection and pumping in low pressure ($<$10s mTorr), high plasma density ($>10^{11}$ cm^{-3}) reactors such as inductively coupled plasma (ICP) tools are less well characterized. These plasma reactors are rapidly becoming the tool of choice for plasma etching and new systems are being developed for deposition.[1–6] Many such systems have gas injection from discrete nozzles and use asymmetric (single sided) pumping under the assumption that at low pressure, transport is primarily by diffusion (as opposed to advection). Under such conditions, gas sources and sinks ideally appear as volume averages, and so their asymmetries should not detrimentally affect the uniformity of reactants to the substrate.

The radial uniformity of reactant fluxes to the substrate in azimuthally symmetric ICP reactors as a function of reactor geometry and coil placement have been computationally investigated in two dimensions in several recent publications.[7–10] In this article, we extend those studies using results from a three-dimensional plasma equipment model.[11] We investigate the consequences of asymmetric pumping and various injection schemes on the azimuthal uniformity of reactants to the substrate in a low pressure, high plasma density ICP reactor operating in Cl$_2$. We find that ion densities and fluxes to the substrate are generally more uniform than their neutral counterparts due to the dominance of ambipolar forces. For species such as Cl, which are relatively unreactive on the walls, the azimuthal asymmetries produced by,

for example, side pumping are 10%–15%, a value which depends on the arrangement of the injection nozzles, gas pressure, and wall reactivity. The model used in this study is described in Sec. II, followed by a discussion of our results in Sec. III. Concluding remarks are in Sec. IV.

II. DESCRIPTION OF THE MODEL

The three-dimensional simulation we have used in this study is based on that described in detail in Ref. 11, and is called the hybrid plasma equipment model (HPEM-3D). HPEM-3D consists of three major modules. The electromagnetic module (EMM) produces the amplitude and phase of inductively coupled fields as a function of (r, θ, z). These fields are then used in the electron energy equation module (EEM) which solves for the average electron energy as a function of position. These values are used to calculate electron transport coefficients and electron impact source functions for inelastic collisional processes. The electron transport coefficients and source functions are subsequently used in the fluid-kinetics module (FKM) where species densities are obtained and Poisson's equation is solved for the electrostatic potential. The resulting densities, electric fields, and conductivities are cycled back to the EMM and EEM; and the sequence is repeated until quasi-steady-state conditions are obtained.

The version of HPEM-3D used in the present study has been improved from that described in Ref. 11. The major improvement is that we additionally employ heavy particle momentum equations in the FKM to account for inertial effects. Heavy particle neutral and ion densities are now obtained from

$$\frac{\partial N_i}{\partial t} = -\nabla \cdot (\mathbf{v}_i N_i) + S_i \tag{1}$$

[a)]Electronic mail: mjk@uiuc.edu

$$\frac{\partial(N_i\mathbf{v}_i)}{\partial t} = q_i\mathbf{E}/m_i - \nabla P_i - \nabla\cdot(N_i\mathbf{v}_i\mathbf{v}_i) - \nabla\cdot\bar{\bar{\tau}}_i$$

$$+ \sum_j N_iN_jk_{ij}(\mathbf{v}_j - \mathbf{v}_i), \qquad (2)$$

where N_i, $\mathbf{v}_i$, and P_i are the density, velocity, and thermo-dynamic pressure of species i, $\bar{\bar{\tau}}$ is the viscosity tensor, S_i is the source of species i due to all collisions, and k_{ij} is the rate coefficient for momentum transfer collisions between species i and j. Slip boundary conditions are employed using the method described by Thompson.[12] We have not solved the species' energy equations, and so assume isothermal conditions throughout the reactor. Poisson's equation is solved for the electric potential using a semi-implicit technique, and acceleration techniques are used to speed the convergence of the solution. Issues related to noncollisional heating[13] have not been addressed in this study and we are not addressing the consequences of applying a substrate bias. The numerical mesh used a (r,θ,z) geometry with 56×60 mesh points in (r,z) planes and 48 azimuthal slices for a total of 161, 280 mesh points.

There is legitimate concern whether fluid equations are adequate to investigate gas flow uniformity at the low pressures of interest. Studies have been performed which compared the results of direct simulation Monte Carlo[14] and fluid simulations in two and three dimensions[15] with experimental measurements at pressures of a few to 10s mTorr in reactors of the type being considered here. The fluid simulations agreed well with experiments and captured the dominant flow features. In this regard, the results we present here likely capture the appropriate systematic trends but also are likely to be a worst case analysis.

To quantify azimuthal asymmetries, we define the asymmetry factor for quantity ϕ as

$$\beta = \max\frac{|\phi(\theta) - \bar{\phi}|}{\bar{\phi}}, \qquad (3)$$

where $\bar{\phi}$ is the average value of ϕ as a function of azimuth at a given radius, and the max function denotes that we take the maximum value of β as a function of both azimuth and radius across the wafer. Smaller values of β are more uniform.

III. CONSEQUENCES OF ASYMMETRIC PUMPING

The system we will investigate is an ICP etching reactor schematically shown in Fig. 1. The antenna is a two-turn coil set on top of a dielectric window. The Si wafer is 20 cm in diameter and is surrounded by an alumina focus ring. To eliminate asymmetries which may result from either transmission line effects in the antenna or the shape of the antenna, we specified that the coil conduction currents be uniform along the entire length of the coil and that the antenna is simply two nested annuli without azimuthal variation. (Issues related to azimuthal asymmetries associated with the antenna are discussed in Ref. 11.) To isolate the effects of gas flow the reactor is otherwise geometrically azimuthally symmetric with the exception of gas injection and pumping. Gas is injected in one of three patterns. The first nozzle ar-
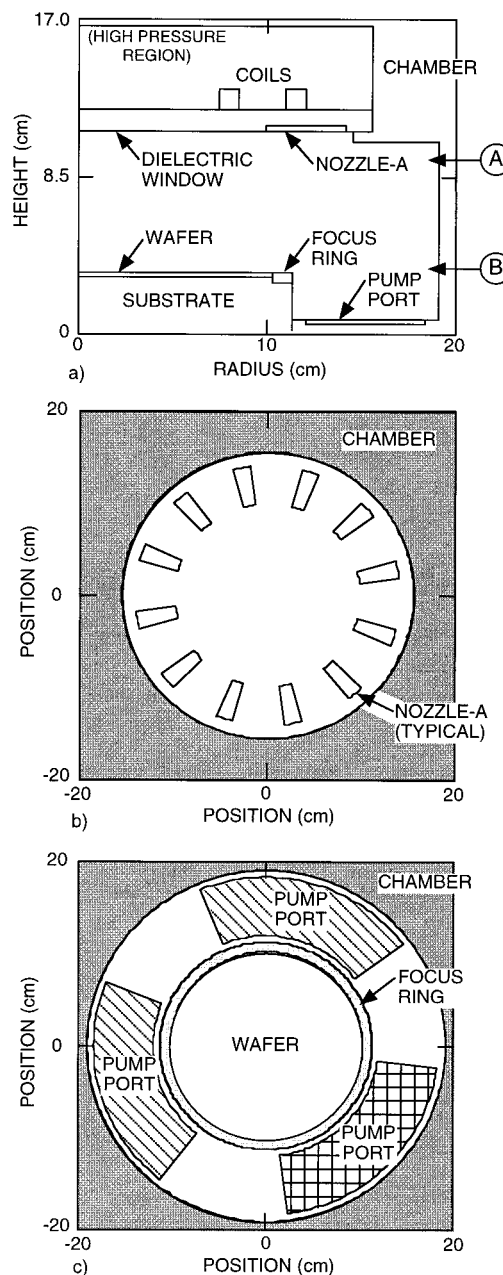

FIG. 1. Schematics of the ICP reactor used in this study. (a) Geometry in (r,z) plane showing the Nozzle-A and pump port locations. The section markers show the height at which densities in the (r,θ) will be shown. (b) View looking up at the bottom of the dielectric window showing a ceiling plan for the layout of Nozzle-A. (c) View looking down at the substrate and pump ports. Asymmetric pumping uses only the cross-hatched port. Symmetric pumping uses all three pump ports.

rangement, shown in Fig. 1 as "Nozzle-A," consists of inlets arrayed uniformly around the outer portion of the dielectric window to a radius corresponding to the edge of the wafer. The gas is injected directly downward. The second and third nozzle arrangements are shown in Fig. 2, labeled "Nozzle-B" and "Nozzle-C". Nozzle-B is a showerhead extending outward to the edge of the wafer and which injects gas directly downward. Nozzle-C is a series of slots which inject gas radially inward. The gas is pumped either symmetrically or asymmetrically. Asymmetric gas pumping is

J. Appl. Phys., Vol. 82, No. 11, 1 December 1997
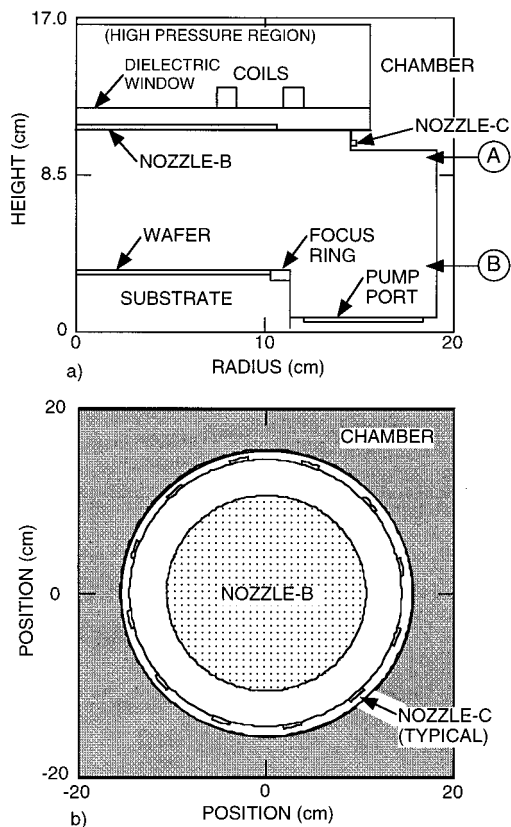
Mark J. Kushner   5313

FIG. 2. Schematics of the ICP reactor showing the alternate inlets; Nozzle-B (a shower head) and Nozzle-C (radially directed jets). (a) Geometry in the (r,z) plane. (b) View looking up at the bottom of the dielectric window showing a ceiling plan for the layouts of Nozzle-B and Nozzle-C.

FIG. 3. Plasma parameters for base case conditions. (10 mTorr Cl_2, 400 W, 150 sccm) (a) Electron source and power deposition, and (b) Cl^- and Cl_2^+ density. The contours are labeled with a percentage of the maximum value noted in each figure.

through a single port shown cross hatched in Fig. 1(c). Symmetric gas pumping is through three evenly spaced ports also shown in Fig. 1(c).

The feedstock gas injected through the nozzles is Cl_2. The reaction mechanism we used includes Cl_2, Cl_2^+, Cl, Cl^+, Cl^-, and electrons, and is listed in Ref. 7. All ions recombine on surfaces with unity probability. Electron impact dissociation (dissociative excitation and dissociative attachment) of Cl_2 produces the reactive species, Cl atoms. The reactive sticking coefficient for Cl on all nonwafer surfaces ($Cl \rightarrow wall \rightarrow Cl_2$) is $\gamma = 0.005$ and on the wafer surface is $\gamma = 0.1$ unless specified otherwise. To simplify the reaction chemistry, we have not included etching reactions by Cl on the wafer but have increased its recombination coefficient on the wafer in recognition of its higher reactivity with that surface. The base case conditions are 10 mTorr, 150 sccm gas flow, 400 W power deposition. The gas temperature is 400 K and ion temperature is 1200 K. Species densities and fluxes will be inspected in the (r,θ) plane at the two heights indicated in Fig. 1(a). Height-A is approximately 1.3 cm below the dielectric window. Height-B is approximately 0.3 cm above the plane of the wafer.

Typical plasma parameters are shown in Fig. 3 for the base case conditions using symmetric pumping with Nozzle-A. The azimuthal variations in these quantities are $\beta < 1\%$ in all cases. The peak ion densities are Cl_2^+ 1.7
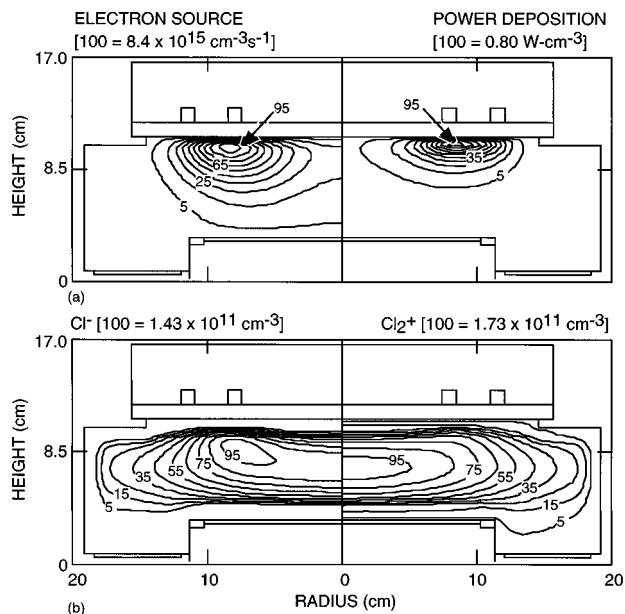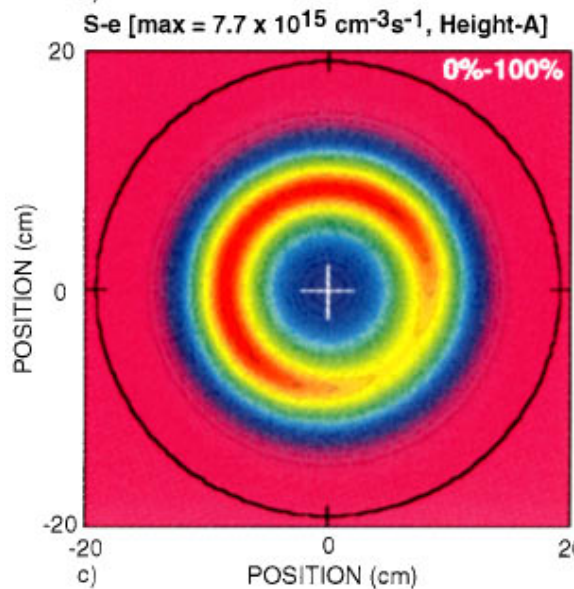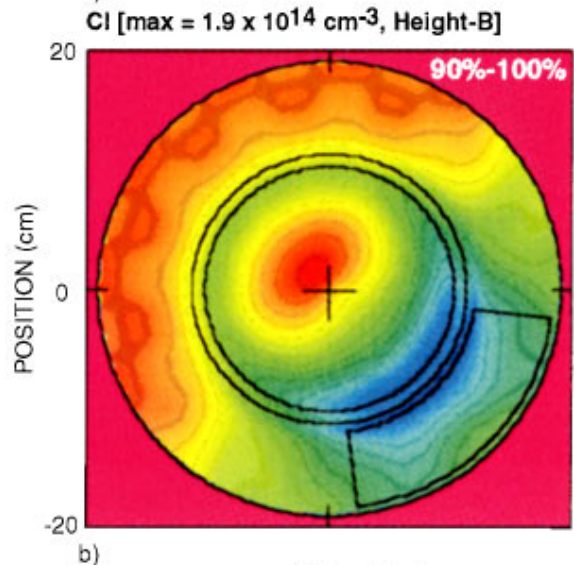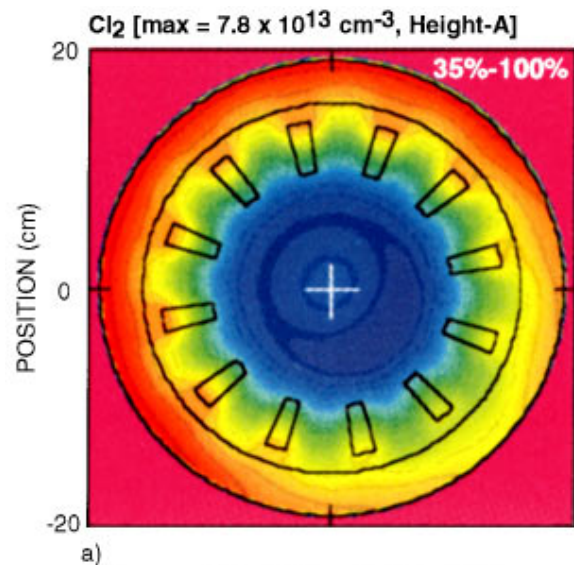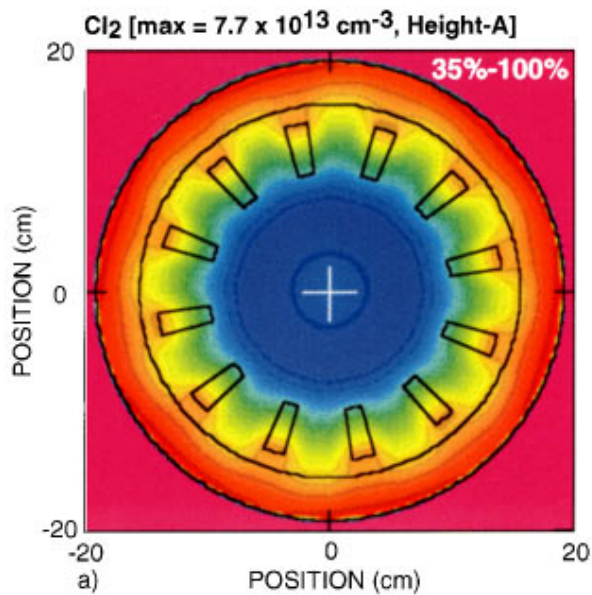
$\times 10^{11}$ cm^{-3}, Cl^+ 7.9×10^{10} cm^{-3}, and Cl^- 1.4 $\times 10^{11}$ cm^{-3} with a peak electron temperature of 3.8 eV and maximum plasma potential of 14.5 V. The Cl^- and Cl_2^+ densities are large here due to the low fractional dissociation resulting from the large flow rate. In ICP reactors using this coil configuration, the power deposition is torroidal in shape with a maximum in radius approximately at the coils and a cm below the window. The electron source has a greater extent, as shown in Fig. 3, due to the large thermal conductivity of the electrons. A discussion of the two-dimensional dependence of power deposition and ion densities in azimuthally symmetric reactors can be found in Refs. 7–10.

The Cl_2 density 1.3 cm below the window (Height-A) and the Cl atom density 0.3 cm above the plane of the wafer (Height-B) are shown in Fig. 4 for symmetric pumping with Nozzle-A. The Cl_2 density is larger in the vicinity of the nozzles, showing a "scallop" pattern, due to the jetting action of the gas injection. The Cl_2 is significantly depleted in the center of the reactor due to electron impact dissociative excitation and dissociative attachment, producing two-Cl and $Cl + Cl^-$, respectively. The large radial pressure gradient resulting from the depletion produces a flux of Cl_2 from the radius of injection to the center, where the Cl_2 is dissociated. Since the ion density has a large outward radial flux, there is also some degree of momentum transfer to the Cl_2 which partly balances the force due to the pressure gradient.

The Cl density at the plane of the wafer is uniform to better than 10% throughout the entire reactor. The density is highest at the center of the wafer due to the centrally located volume sources of Cl by electron impact dissociation of Cl_2, and sinks at the walls. The low reactive sticking coefficient and large mobility of the Cl atoms tend to homogenize local sources and sinks of Cl, producing a high degree of unifor-

                                                                 Mark J. Kushner

Cl₂ [max = 7.7 x 10¹³ cm⁻³, Height-A]

Cl₂ [max = 7.7 × 10¹³ cm⁻³, Height-A]

Cl₂ [max = 7.8 x 10¹³ cm⁻³, Height-A]

Cl₂ [max = 7.8 × 10¹³ cm⁻³, Height-A]

Cl [max = 1.9 x 10¹⁴ cm⁻³, Height-B]

Cl [max = 1.9 × 10¹⁴ cm⁻³, Height-B]

S-e [max = 7.7 x 10¹⁵ cm⁻³s⁻¹, Height-A]

FIG. 4. Chlorine densities using Nozzle-A inlets and symmetric pumping. (a) Cl₂ density at Height-A and (b) Cl density at Height-B. The maximum densities are shown at the top of each figure. In order to emphasize the azimuthal asymmetries, the ranges of densities plotted are over the minimum and maximum densities occurring at each height. The ranges of densities plotted (as a percentage of the maximum value) are noted at the top right in each figure. The cross denotes the center of the wafer for reference.

FIG. 5. Chlorine densities and electron source using Nozzle-A inlets and asymmetric pumping. (a) Cl₂ density at Height-A, (b) Cl density at Height-B, and (c) electron source function at Height-A. The labeling scheme is the same as in Fig. 4. The Cl₂ and Cl densities show asymmetries due to the single sided pumping. The maximum in the Cl density is shifted due to depletion of Cl in the direction of the pump. The electron source function has a minimum in the direction of the pump due to a small decrease in electron temperature.

mity. The azimuthal variation of the Cl atom density resulting from azimuthal asymmetries in either injection or pumping is less than $<1\%$ ($\beta = 0.2\%$) across the wafer. There is a small increase in Cl density in the direction of the pump ports. This appears to be a consequence of Cl, which is depleted by reaction on the wafer, being replenished from larger heights by a flux which is directed towards the pump ports. This behavior differs from the asymmetric pumping case. Note also that there is a small scalloping of the Cl density beyond the radius of the wafer. This scalloping results from momentum transfer from Cl_2 whose jetting persists from the injection nozzles to the plane of the wafer.

The Cl_2 density below the window and Cl atom density above the wafer are shown in Fig. 5 for Nozzle-A and asymmetric pumping. The total electron source function due to ionization, attachment and recombination is also shown at the same height as for Cl_2. The Cl_2 density displays a scalloped appearance due to the discrete jetting from the nozzles, but now also shows a moderate side-to-side azimuthal variation. The Cl_2 is maximum opposite the pump port and lowest above the pump port. Although Cl_2 is dissociated by 2/3 in the center of the plasma, there is still evidence of a side-to-side azimuthal variation in its density within the depleted core. The Cl atom density at the plane of the wafer also shows a side-to-side azimuthal variation of $\approx 10\%$ across the reactor and about half that across the wafer ($\beta \approx 4.0\%$). The peak in the Cl density is offset from the center of the wafer and is shifted away from the pump port. The net gas flow is now across the wafer towards the pump while dissociation of Cl_2 is dominantly at higher heights. The sweeping of Cl atoms across the wafer, where they are consumed, results in a side-to-side depletion of the Cl towards the pump. The increase in flow speed and reduction in pressure near the pump also is a contributing factor. Vestiges of momentum transfer from the Cl_2 jets (in the form of scalloping of the Cl atom density) is still evident on the side opposite the pump port but have been masked near the pump port.

In the majority of cases investigated, charged particle densities and fluxes were azimuthally more uniform than their neutral counterparts. Whether this observation is general critically depends on the particulars of the ion generation and loss processes. For example, an ion which is produced from a single azimuthally asymmetric neutral species and which is quickly neutralized will have a similarly asymmetric profile. If we assume that sources are uniform, then the uniformity of charged species, and their azimuthal symmetry in particular, are largely determined by the ambipolar or applied electric fields which dominate their transport to surfaces where, with rare exception, they are neutralized. The direction and magnitude of ambipolar electric fields are determined by the uniformity of the ion sources and the symmetry of the reactor. Therefore if the electron impact sources of ions are symmetric and the reactor is symmetric then the ion fluxes will be largely symmetric.

The symmetry of gas injection and pumping, and the symmetry of the neutral species can, however, impact the symmetry of the ions in at least two ways. First, asymmetric neutral densities may contribute to asymmetric ion sources
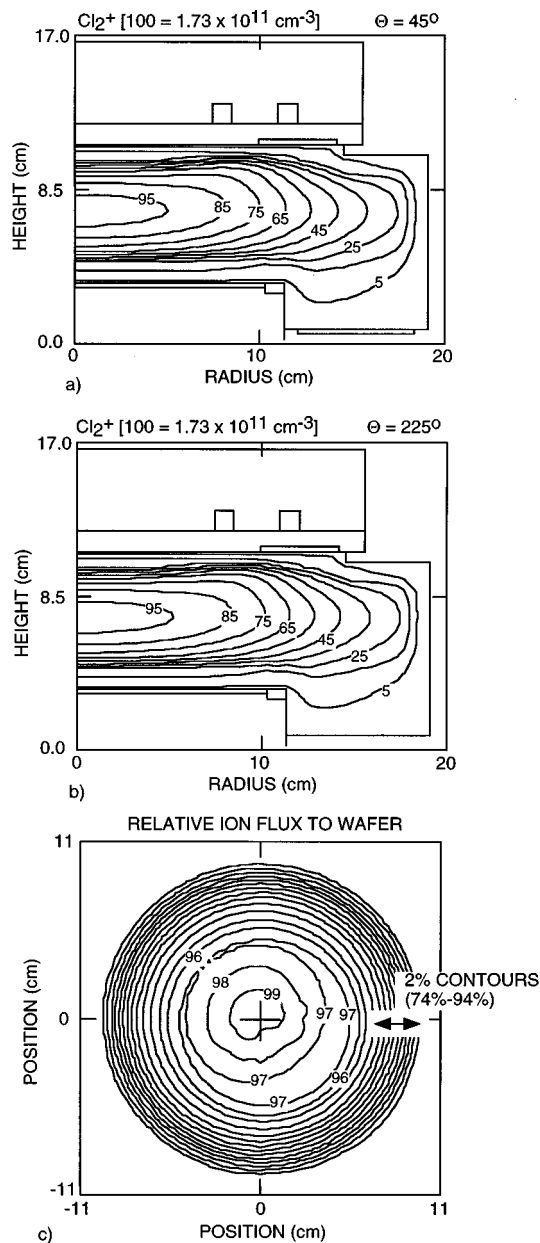

FIG. 6. Ion properties using Nozzle-A inlets and asymmetric pumping. (a) Cl_2^+ density in the (r,z) plane cutting through the center of the pump port. (b) Cl_2^+ density in the (r,z) plane 180° opposed to the pump port. (c) Total positive ion flux to the wafer. The contours are labeled with the percent of the maximum value. In all cases studied, the ion densities and fluxes were more azimuthally symmetric than their neutral counterparts.

by electron impact collisions and to asymmetric rates of ion production or loss by ion-molecule reactions (such as $Cl^+ + Cl_2 \rightarrow Cl + Cl_2^+$). Asymmetries in neutral densities which have high spatial frequencies are not particularly important in this regard (such as that found by the inlet nozzles in the base case) because of the high transverse mobility of ions which quickly mitigate these gradients. The degree to which asymmetries in electron impact source functions affect the uniformity of ion fluxes is discussed in Ref. 11 in the context of antenna design in ICP systems and this effect can be significant. Second, asymmetric neutral fluxes may pro-
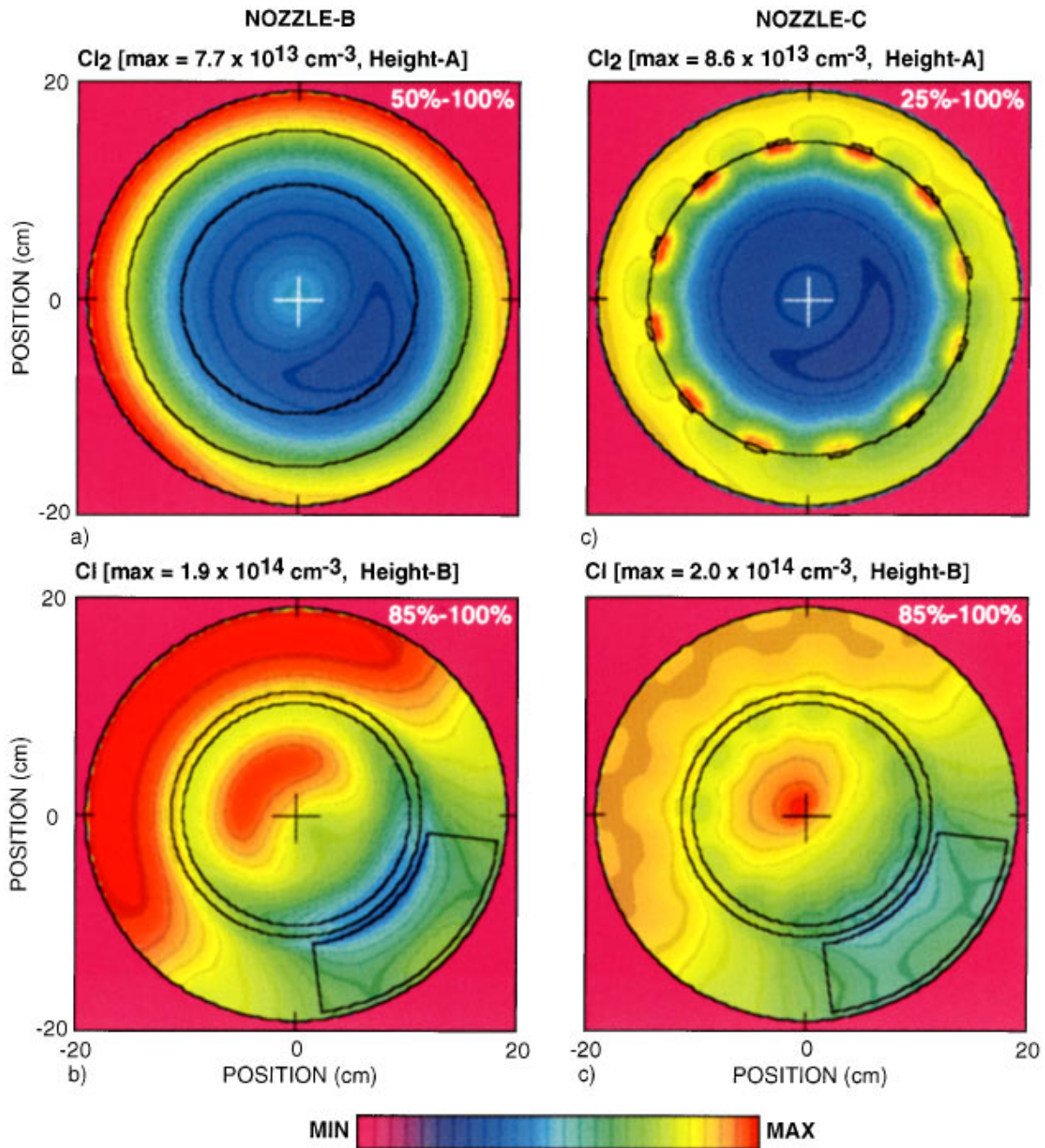
Mark J. Kushner

NOZZLE-B

Cl_2 [max = 7.7×10^{13} cm^{-3}, Height-A]

50%-100%

a)

Cl [max = 1.9×10^{14} cm^{-3}, Height-B]

85%-100%

b)

NOZZLE-C

Cl_2 [max = 8.6×10^{13} cm^{-3}, Height-A]

25%-100%

c)

Cl [max = 2.0×10^{14} cm^{-3}, Height-B]

85%-100%

c)

MIN ▮▮▮▮▮▮▮▮▮▮▮▮ MAX

FIG. 7. Chlorine densities using the showerhead (Nozzle-B, left column) and radial jet (Nozzle-C, right column) inlets and asymmetric pumping. (a) Cl_2 density at Height-A (Nozzle-B), (b) Cl density at Height-B (Nozzle-B), (c) Cl_2 density at Height-A (Nozzle-C), and (b) Cl density at Height-B (Nozzle-C). The labeling scheme is the same as in Fig. 4. The showerhead (Nozzle-B) produces a larger asymmetry and side-to-side variation in Cl density at the wafer.

duce asymmetries in ion fluxes due to momentum transfer reactions between the neutrals and ions, or by charge exchange to neutrals which already have large asymmetries in their fluxes, which are then imprinted on the charge exchange ion.

The electron source function for the base case at Height-A is shown in Fig. 5(c). Recall that the antenna currents have been forced to be azimuthally symmetric (unlike those discussed in Ref. 11), and so the electric field launched into the plasma is azimuthally symmetric. Nevertheless, there is an azimuthal asymmetry in the electron source function ($\beta \approx 19\%$) being smaller adjacent to the pump port. This

asymmetry largely results from a small local minimum in the electron temperature (<0.1 eV) at that location, a consequence of a small change in the local ratio of Cl/Cl_2. Since rate coefficients for electron impact events having high threshold energies, such as ionization, are most sensitive to small changes in electron temperature, there is a magnified effect on the electron source as shown in Fig. 5(c). This reduction is further magnified by an electron attachment rate which increases with decreasing temperature. It is difficult, however, to see large azimuthal variations in the ion properties. For example, the Cl_2^+ densities in the (r,z) plane for an azimuth at the center of the pump port and an azimuth di-

J. Appl. Phys., Vol. 82, No. 11, 1 December 1997
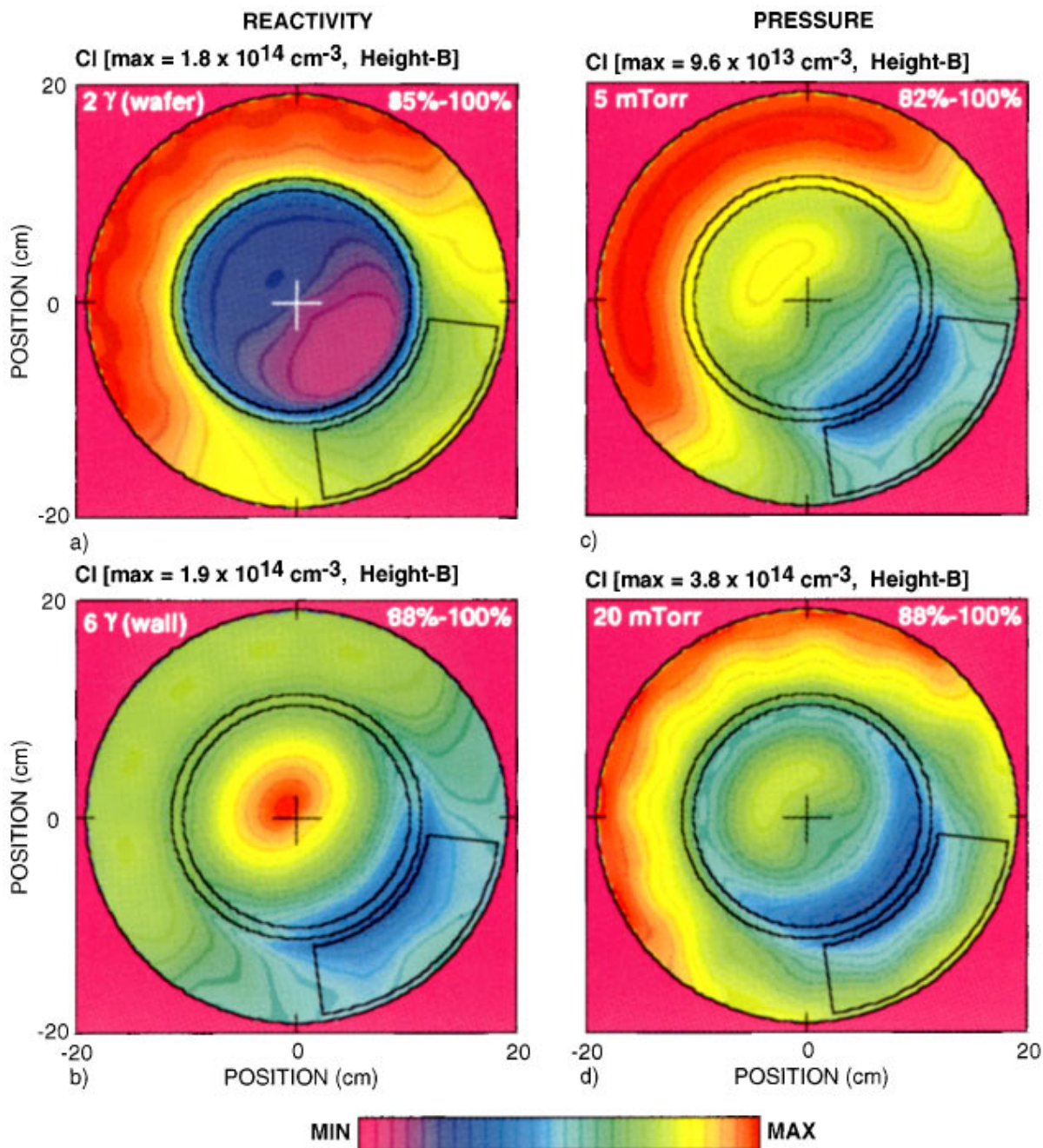
Mark J. Kushner   5317

FIG. 8. Cl densities using Nozzle-A with asymmetric pumping at the wafer (Height-B). (a) Higher sticking coefficient for Cl on the wafer, (b) Higher sticking coefficient for Cl on the walls, (c) 5 mTorr, 200 W, 75 sccm, (d) 20 mTorr, 800 W, 300 sccm. The labeling scheme is the same as in Fig. 4.

rectly opposite the pump port are shown in Fig. 6, as is the total ion flux to the wafer. The Cl_2^+ densities are nearly identical, varying on only the few percent level in spite of the asymmetric ion source. The total ion flux to the wafer, shown in Fig. 6(c), has a small azimuthal asymmetry. This asymmetry is a shallow minimum, corresponding to the minimum in ionization rate above it occurring in the electromagnetic skin depth [Fig. 5(c)].

The manner of gas injection also has an influence on the azimuthal asymmetry of the Cl flux. For example, the densities of Cl_2 (Height-A) and Cl (Height-B) for the showerhead (Nozzle-B) and radial jet (Nozzle-C) inlets are shown in Fig. 7. The Cl_2 density using the shower head is less depleted in the center of the reactor due to the downward injection of Cl_2 through the power deposition region which rapidly replenishes the dissociated feedstock gas. The depletion is more severe in the direction of the pump port thereby producing an asymmetry. The Cl_2 density with the radial jets shows, as expected, more scalloping in its density which produces an azimuthal asymmetry with high spatial frequency. On the average, however, the Cl_2 density appears more symmetric. The Cl densities above the wafer show similar trends, however, the qualitative distributions are different. In the case of the showerhead nozzle, the maximum of the Cl atom density is offset to a larger radius producing a greater side-to-side

variation compared to the base case although β is similar. In the case of the discrete nozzles, there are again variations having high spatial frequency, which produce a larger β (4.2%); however the azimuthal symmetry is, on average, superior to that using the showerhead. The maximum in the Cl density occurs nearer the center of the wafer while the side-to-side variation in density is less severe.

The azimuthal asymmetry of Cl atoms is, in part, determined by their reactivity. For example, the Cl density is shown in Fig. 8(a) at Height-B for the base case conditions except that the reactive sticking coefficient for Cl on the wafer was increased from 0.1 to 0.2. Comparing those results to the base case [Fig. 4(b)], we find a much reduced density of Cl above the wafer while the azimuthal asymmetry beyond the edge of the wafer subtends a larger angle. Due to the higher reactivity of the Cl atoms as they flow across the wafer in the direction of the pump, the azimuthal asymmetry worsens. The Cl density obtained while increasing the wall sticking coefficient from 0.005 to 0.03 is shown in Fig. 8(b). While quantitatively the symmetry is only marginally improved from the base case ($\beta = 3.7\%$), qualitatively, the Cl density appears more symmetric. The peak density is closer to the center of the wafer and contours are more circular. The apparent improvement in symmetry results from the wall loss beginning to compete with loss of Cl by pumping. Since the wall loss is azimuthally symmetric, as is the source of Cl atoms, the symmetry of the Cl flux to the wafer is improved.

Gas pressure also influences the azimuthal symmetry. In order to isolate the effect of pressure, cases were run at 5 mTorr (200 W, 75 sccm) and 20 mTorr (800 W, 300 sccm) while keeping residence time, and fractional dissociation nearly the same. The Cl atom densities at Height-B are shown in Fig. 8 for these cases. In principle, keeping these conditions constant should produce nearly the same Cl density profiles at the wafer using a fluid model. We see, however, a significant qualitative difference. Although the region of Cl depletion near the pump is less pronounced at low pressure, the side-to-side asymmetry is greater. We attribute this effect to the depletion by reaction with the wafer of the smaller number of Cl atoms at the lower pressure. The Cl atom density at 20 mTorr retains a greater overall azimuthal symmetry but has more high spatial frequency asymmetries. For these process conditions, the azimuthal symmetry of Cl is qualitatively best at about 10 mTorr.

We have seen that neutral reactant fluxes do not necessarily improve when lowering the operating pressure, at least for these conditions. That conclusion ultimately depends on the details of the reaction chemistry (wall and volume). We can, however, conclusively state that the symmetry of ion fluxes to the wafer do improve by lowering gas pressure. This trend is demonstrated in Fig. 9 where ion fluxes to the wafer are shown for the 5 and 20 mTorr cases. The ion flux at 5 mTorr is essentially azimuthally symmetric while that at 20 mTorr shows significant azimuthal asymmetries. The higher mobility of ions, higher plasma potential, and larger ambipolar fields at the lower pressure, all contribute to the high degree of azimuthal symmetry. Another important consideration is the scaling of the discharge response time τ with pressure P. This scaling, for constant E/N, is $P\tau$
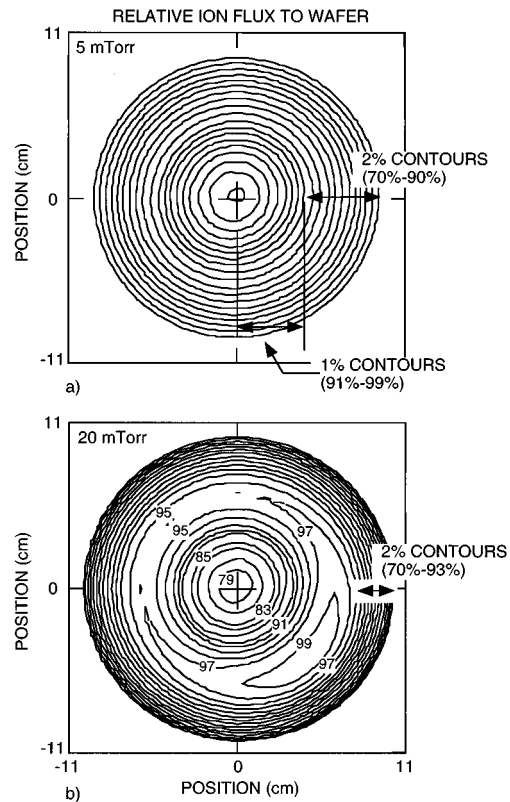

FIG. 9. Ion fluxes to the wafer for (a) 5 mTorr and (b) 20 mTorr. In all cases studied, the azimuthal symmetry of the ion flux improved at lower pressures.

= constant. At higher pressures, the plasma responds to small perturbations more rapidly, an effect which is typically exponential. Therefore, for all other parameters being constant, higher pressure plasmas will have more asymmetric ion fluxes simply because the plasma responds more quickly to small perturbations.

IV. CONCLUDING REMARKS

The consequences of asymmetric pumping and various inlet geometries have been computationally investigated for an ICP reactor operating in Cl_2 over pressures of 5–20 mTorr. Due to its low reactivity on surfaces, Cl atom densities are fairly uniform throughout the reactor. Systematic azimuthal asymmetries can be produced by side pumping but these variations are, in general, $<10\% - 15\%$ for the conditions of interest. In all cases, the spatial distribution of ion densities and fluxes were more uniform than their neutral counterparts. This observation results from the dominance of ambipolar transport in determining their fluxes, a quantity which depends on the symmetry of the ion sources and the shape of the container, but is not particularly sensitive to pumping asymmetries. The scaling of azimuthal symmetry of neutral reactants with pressure is less clear. Species with high wall reactivity tend to be more azimuthally symmetric though higher wafer reactivity produces less symmetric fluxes. In all cases, though, the ion flux symmetry improved with decreasing pressure. Generalizing these results, one can expect a high degree of azimuthal symmetry when side

J. Appl. Phys., Vol. 82, No. 11, 1 December 1997

Mark J. Kushner   5319

pumping or lowering pressure for plasma processes which are ion driven or in the ion-starved regime where the rate of processing is limited by the ion availability. This would include oxide and most polysilicon etch processes. Selectivity, however, which may depend on details of the neutral flux of radicals producing passivating polymerization, will be more sensitive to asymmetric pumping and pressure variation. Processes which are neutral driven will be in general more sensitive to the symmetry of pumping and injection.

[1] J. Hopwood, Plasma Sources Sci. Technol. **3**, 640 (1994).

[2] J. H. Keller, J. C. Forster, and M. S. Barnes, J. Vac. Sci. Technol. A **11**, 2487 (1993).

[3] M. S. Barnes, J. C. Forster, and J. H. Keller, Appl. Phys. Lett. **62**, 2622 (1993).

[4] R. Patrick, R. Schoenborn, and H. Toda, J. Vac. Sci. Technol. A **11**, 1296 (1993).

[5] L. J. Mahoney, A. E. Wendt, E. Barrios, C. J. Richards, and J. L. Shohet, J. Appl. Phys. **76**, 2041 (1994).

[6] T. H. Ahn, K. Nakamura, and H. Sugai, Plasma Sources Sci. Technol. **5**, 139 (1996).

[7] P. L. G. Ventzek, M. J. Grapperhaus, and M. J. Kushner, J. Vac. Sci. Technol. B **12**, 3118 (1994).

[8] R. A. Stewart, P. Vitello, D. B. Graves, E. F. Jaeger, and L. A. Berry, Plasma Sources Sci. Technol. **4**, 36 (1995).

[9] G. Dipeso, V. Vahedi, D. W. Hewett, and T. D. Rognlien, J. Vac. Sci. Technol. A **12**, 1387 (1994).

[10] D. L. Lymberopoulos and D. Economou, Trans. Plasma Sci. **23**, 573 (1995).

[11] M. J. Kushner, W. Z. Collison, M. J. Grapperhaus, J. P. Holland, and M. S. Barnes, J. Appl. Phys. **80**, 1337 (1996).

[12] P. A. Thompson, *Compressible Fluid Dynamics* (McGraw-Hill, New York, 1972), Chap. 2.

[13] V. I. Kolobov, D. P. Lymberopoulos, and D. J. Economou, Phys. Rev. E **55**, 3408 (1997).

[14] P. K. Shufflebotham, T. J. Bartel, and B. Berney, J. Vac. Sci. Technol. B **13**, 1862 (1995).

[15] V. Singh, B. Berney, and A. Krishnan, J. Vac. Sci. Technol. A **14**, 1252 (1996).